SCIENTIFIC JOURNAL
EARTH'S CRYOSPHERE

Earth's Cryosphere, 2016, vol. XX, No. 3, pp. 59–65 **http://earthcryosphere.ru/**

GAS HYDRATE FORMATION

GAS HYDRATE FORMATION IN POROUS ICE-RICH METHANE RESERVOIRS UPON INJECTION OF CARBON DIOXIDE: FORWARD MODELING

M.K. Khasanov[1], N.G. Musakaev[2,3]

[1]Sterlitamak Branch of Bashkir State University, 49, Lenina ave., Sterlitamak, 453103, Russia; hasanovmk@mail.ru
[2] Tyumen Branch of Khristianovich Institute of Theoretical and Applied Mechanics, SB RAS, 74, Taymirskaya str., Tyumen, 625026, Russia; musakaev@ikz.ru
[3]Tyumen State University, 6, Volodarskogo str., Tyumen, 625003, Russia; musakaev68@yandex.ru

Formation of CO_2 hydrate during injection of carbon dioxide into porous ice-rich methane reservoirs is studied using forward modeling in terms of heat and mass transfer. The obtained solutions describe the temperature and pressure patterns in the sediments and show that gas hydrate forms at three different regimes depending on the injected gas pressure and reservoir permeability. The results have implications for strategies of subsurface CO_2 sequestration and safe disposal as gas hydrate in porous reservoirs, as well as for the conditions of CO_2 hydrate stability.

Carbon dioxide sequestration, gas hydrate, porous reservoirs, permafrost, methane

INTRODUCTION

Rapid growth of atmospheric carbon dioxide (CO_2) responsible for the greenhouse effect has been a focus of major recent concern. It was suggested to reduce greenhouse emissions by capture and sequestration of CO_2 in deep sedimentary formations [*Oldenburg et al., 2001; Benson and Cole, 2008*]. As an alternative to long-term fluid carbon dioxide storage fraught with emission risks, permanent underground CO_2 disposal is possible by solid clathrate hydrate formation [*Jadhawar et al., 2006*], in unfrozen sediments, as well as in permafrost [*Chuvilin and Guryeva, 2009; Duchkov et al., 2009*]. Frozen and ice-rich rocks are commonly poorly permeable for gas though may contain zones of high permeability [*Olovin, 1993*]. Low permeability of the frozen cap and stability of gas hydrates at low temperatures secure sequestration of CO_2 in permafrost [*Duchkov et al., 2009*]. Formation of gas hydrates actually increases the capacity of CO_2 reservoirs because, at the same conditions, the amount of gas in a unit volume of hydrate far exceeds that of free gas [*Makogon, 1974*]. On the other hand, gas hydrate formation produces hydrate plugs around boreholes and impedes further gas flow, which poses engineering problems. In this respect, formation of gas hydrates in ice-rich rocks requires a special study.

Modeling gas hydrate formation is additionally motivated by poor understanding of deposition mechanisms of hydrate-bearing sediments in permafrost and on the Arctic shelf [*Yakushev et al., 2003*]. Mathematical modeling of the injection of gas into porous reservoirs and its conversion to hydrates can shed light on some deposition patterns of continental hydrate-bearing sediments.

Experiments on CO_2 hydrate formation in porous media containing ice and water [*Chuvilin et al., 2007; Chuvilin and Guryeva, 2008, 2009; Komai et al., 2008*] show that gas hydrates can accumulate in water-saturated rocks, as well as in those partly saturated with ice, while the process decays more rapidly in the former case. Note that those and other similar experiments were applied to small samples under isothermal and isobaric conditions. Meanwhile, gas hydrate formation in small samples is constrained by the kinetics of the process, unlike the natural reservoirs where it depends more on heat and mass transfer in the porous medium itself.

Gas hydrate formation in water-bearing reservoirs of methane (CH_4) was modeled previously [*Shagapov et al., 2008, 2011, 2015; Khasanov et al., 2010*] assuming injection of the same gas. The model of *Tsypkin* [*2014*] simulated injection of CO_2 into methane reservoirs. We now investigate injection of free CO_2 into a frozen methane reservoir and the ensuing formation of gas hydrates.

Heat and mass transfer in a porous ice-rich methane reservoir upon injection of CO_2

We obtain a 1D forward model for CO_2 injection into a porous ice-rich (with the initial saturation S_{i0})

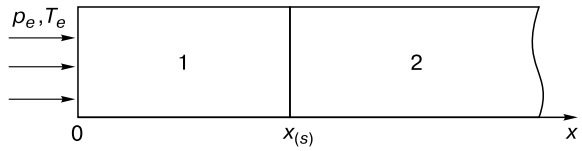

Fig. 1. Model of carbon dioxide injection.

1 – saturation with CO_2 hydrate and free carbon dioxide; 2 – saturation with ice and methane; $x_{(s)}$ is phase boundary; p_e and T_e are, respectively, pressure and temperature of injected carbon dioxide.

methane reservoir impermeable from above and from below, which occupies the halfspace $x > 0$. Let the initial pressure (p_0) and temperature (T_0) be constant throughout the reservoir and thermodynamically allow coexistence of methane and ice in the pore space. Assume that gaseous CO_2 is injected from the left-hand reservoir edge ($x = 0$) where constant pressure and temperature (p_e and T_e, respectively) are maintained such to allow free CO_2 to be mixed with its hydrate (Fig. 1).

The conditions at which gas hydrates (of carbon dioxide and methane) can exist are shown in the phase diagram of Fig. 2 [*Istomin and Yakushev, 1992*] where the curves *glh* and *gih* refer to three-phase equilibrium "gas–liquid–hydrate" and "gas–ice–hydrate" and the curves *il* and *lg* refer to two-phase equilibrium "ice–water" and "liquid–gas", respectively. The subscripts 1 and 2 refer, respectively, to CO_2 and CH_4 in the gas, liquid, and hydrate forms. Thus, the initial pressure and temperature values are below the g_2ih_2 curve (in the field of the ice-methane mixture) while the values for the injected CO_2 lie between the curves g_1ih_1 and l_1g_1 (in the field of mixed gaseous and hydrate CO_2).

The temperatures and pressures for the three-phase equilibrium "gas–liquid–hydrate" are related as [*Byk et al., 1980*]:

$$T = T_0 + T_* \ln\left(\frac{p}{p_{s0}}\right), \qquad (1)$$

where p_{s0} is the equilibrium pressure corresponding to the temperature T_0; T_* is the empirical parameter depending on the gas hydrate composition and on the H_2O state.

Mass and heat transfer by infiltration is much more rapid than that by diffusion. In this respect, we assume, like *Tsypkin* [*2014*], that the two gases do not mix and that the front of methane expulsion by carbon dioxide is stable, proceeding from the mostly laminar flow behavior in porous media and greater viscosity of CO_2 than CH_4. Then, CO_2 injection into a methane reservoir (Fig. 1) produces two domains in which the pores are filled with free CO_2 + CO_2 hydrate (proximal domain 1) and methane + ice (dis-

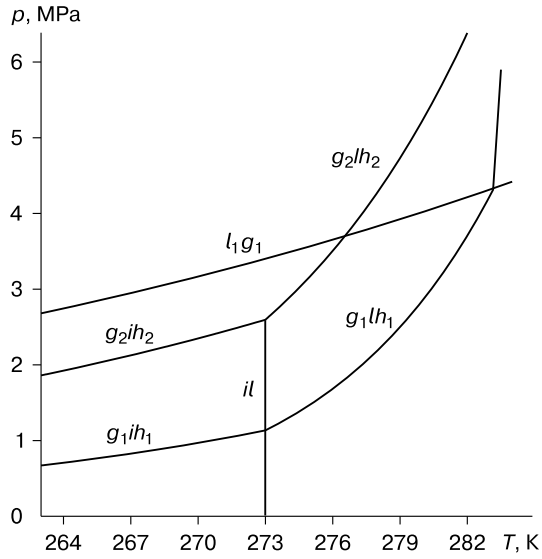

Fig. 2. Phase diagrams of CO_2–H_2O and CH_4–H_2O systems.

glh and *gih* are curves of three-phase equilibrium "gas–liquid–hydrate" and "gas–ice–hydrate"; *il* and *lg* are curves of two-phase equilibrium "ice–water" and "liquid–gas"; subscripts 1 and 2 refer to CO_2 and CH_4, respectively (free gas and its hydrate).

tant domain 2). With these assumptions, all CO_2 hydrate forms at the moving front between the two domains under the control of mass transfer in a porous medium.

The suggested model is valid for the case when gas hydrate formation is constrained by heat and mass transfer in porous media rather than by the kinetics of the process as it has long characteristic times corresponding to a large size of the reservoir. Note that the mole H_2O content in a unit volume of ice is about 15 % higher than in a unit volume of CO_2 hydrate, i.e., the volume changes when gas hydrate forms. This change produces pores and cracks in the gas-hydrate zone between gas and ice which thus come again into immediate contact.

The heat and mass transfer during CO_2 injection into a porous bed is modeled with the following assumptions: (1) the porous rocks and the saturating material (gas and hydrate) have the same temperature; (2) CO_2 hydrate is a two-component system with the CO_2 weight fraction G; (3) the rock skeleton and the gas hydrate are incompressible, and the porosity m is constant.

The system of equations describing infiltration and heat transfer in a porous medium includes the conservation equations and Darcy's law. In the 1D case, with the above assumptions, this system for each domain is [*Khasanov et al., 2010; Shagapov et al., 2015*]

$$\frac{\partial}{\partial t}\left(\rho_{g(j)} m S_{g(j)}\right) + \frac{\partial}{\partial x}\left(\rho_{g(j)} m S_{g(j)} v_{g(j)}\right) = 0, \; j = 1, 2,$$

$$\frac{\partial}{\partial t}\left(\rho c T_{(j)}\right) + \rho_{g(j)} c_{g(j)} m S_{g(j)} v_{g(j)} \frac{\partial T_{(j)}}{\partial x} = \frac{\partial}{\partial x}\left(\lambda \frac{\partial T_{(j)}}{\partial x}\right), \quad (2)$$

$$m S_{g(j)} v_{g(j)} = -\frac{k_{g(j)}}{\mu_{g(j)}} \frac{\partial p_{(j)}}{\partial x},$$

where ρ_g, v_g, k_g, c_g, and μ_g are, respectively, the true density, velocity, permeability, specific heat, and dynamic viscosity of the gas phase; S_g is the gas saturation; p is the pressure; T is the temperature; ρc is the volumetric specific heat of rocks; λ is the thermal conductivity of rocks. Hereafter the subscripts *sk*, *g*, *i*, and *h* refer to the parameters of rocks (skeleton), gas, ice, and hydrate, respectively; the subscripts 1 and 2 in braces refer to the respective parameters in domains 1 and 2 (Fig. 1).

Gas density is related with pressure and temperature by the Clapeyron–Mendeleev equation:

$$p_{(j)} = \rho_{g(j)} R_{g(j)} T_{(j)}, \; j = 1, 2,$$

where R_g is the gas constant.

The volumetric specific heat ρc and the thermal conductivity λ of rocks are

$$\rho c = (1-m)\rho_{sk} c_{sk} + m \sum_{j=g,i,h} S_j \rho_j c_j,$$

$$\lambda = (1-m)\lambda_{sk} + m \sum_{j=g,i,h} S_j \lambda_j,$$

where ρ_j, c_j, λ_j, and S_j ($j = sk, g, i, h$) are, respectively, the true density, the specific heat, the thermal conductivity, and the saturation of the phases. The values ρc and λ are assumed to be constant throughout the reservoir as the rock skeleton has the greatest contribution.

Proceeding from the Kozeny equation [*Barenblatt et al., 1982*], gas permeability (k_g) is related with gas saturation (S_g) and absolute permeability (k_0) as

$$k_g = k_0 S_g^3.$$

The conditions at the boundary between domains 1 and 2, with regard to heat and mass balance [*Nigmatulin, 1987*], are

$$\begin{aligned} m S_{g(1)} \rho_{g(1)} \left(v_{g(1)} - \dot{x}_{(s)}\right) &= m S_h \rho_h G \dot{x}_{(s)}, \\ m S_{g(2)} \rho_{g(2)} \left(v_{g(2)} - \dot{x}_{(s)}\right) &= 0, \\ m S_h \rho_h (1-G) \dot{x}_{(s)} &= m S_{i0} \rho_i \dot{x}_{(s)}, \\ \lambda \frac{\partial T_{(1)}}{\partial x} - \lambda \frac{\partial T_{(2)}}{\partial x} &= m S_h \rho_h L_h \dot{x}_{(s)}, \end{aligned} \quad (3)$$

where ρ_h and L_h are, respectively, the density of CO_2 hydrate and the heat of its formation; S_h is the hydrate saturation; ρ_i is the ice density; $\dot{x}_{(s)}$ is the speed of the moving phase transition front; G is the fraction of CO_2 in gas hydrate. The temperature and the pressure are assumed to be continuous along this boundary. Hereafter the subscript *s* refers to parameters at the boundary between domains 1 and 2.

Hydrate saturation of domain 1 can be inferred from the third equation in system (3):

$$S_h = \frac{\rho_i S_{i0}}{\rho_h (1-G)}.$$

The initial and boundary conditions of the problem are

$t = 0$: $S_i = S_{i0}$, $T = T_0$, $p = p_0$ ($x \geq 0$);

$x = 0$: $T = T_e$, $p = p_e$ ($t > 0$).

Based on system (2), the pressure conductivity and thermal diffusivity equations can be written as

$$\frac{\partial p_{(j)}^2}{\partial t} = \chi_{(j)}^{(p)} \frac{\partial}{\partial x}\left(\frac{\partial p_{(j)}^2}{\partial x}\right), \; j = 1, 2,$$

$$\frac{\partial T_{(j)}}{\partial t} = \chi^{(T)} \frac{\partial}{\partial x}\left(\frac{\partial T_{(j)}}{\partial x}\right) + \chi^{(T)} \frac{c_{g(j)} k_{g(j)} \rho_{g0}}{\lambda \mu_{g(j)}} \frac{\partial p_{(j)}}{\partial x} \frac{\partial T_{(j)}}{\partial x},$$

where $\chi_{(j)}^{(p)} = \dfrac{k_{g(j)} p_{(j)}}{\mu_{g(j)} m S_{g(j)}}$; $\chi^{(T)} = \dfrac{\lambda}{\rho c}$.

Self-similar solution for temperature and pressure patterns

For analytical solutions, we introduce the self-similar variable $\xi = x \Big/ \sqrt{\chi^{(T)} t}$ which allows writing the pressure conductivity and thermal diffusivity equations in the ordinary differential form:

$$-\xi \frac{dp_{(j)}^2}{d\xi} = 2\eta_{(j)} \frac{d}{d\xi}\left(\frac{dp_{(j)}^2}{d\xi}\right), \; j = 1, 2,$$

$$-\xi \frac{dT_{(j)}}{d\xi} = \frac{\mathrm{Pe}_{(j)}}{p_0^2} \frac{dp_{(j)}^2}{d\xi} \frac{dT_{(j)}}{d\xi} + 2 \frac{d}{d\xi}\left(\frac{dT_{(j)}}{d\xi}\right),$$

where $\eta_{(j)} = \dfrac{\chi_{(j)}^{(p)}}{\chi^{(T)}}$; $k_{g(j)} = k_0 S_{g(j)}^3$; and

$\mathrm{Pe}_{(j)} = \dfrac{\rho_{g0} c_{g(j)}}{\lambda} \dfrac{k_{g(j)} p_0}{\mu_{g(j)}}$ is the Péclet number.

The pressure conductivity equation is nonlinear as the coefficient before the second-order derivative includes the unknown function $p_{(j)}$. An approximate analytical solution can be obtained using Leibenson's linearization [*Basniev et al., 1993*], i.e., the variable pressure $p_{(j)}$ in the pressure conductivity $\chi_{(j)}^{(p)}$ is assumed to be constant and equal to the initial reservoir pressure p_0.

Integrating the pressure conductivity and thermal diffusivity equations gives the pressure and temperature patterns within each domain:

$$\begin{cases} p_{(1)}^2 = p_{(s)}^2 + \left(p_e^2 - p_{(s)}^2\right)\int\limits_{\xi}^{\xi_{(s)}} \exp\left(-\frac{\xi^2}{4\eta_{(1)}}\right)d\xi \left[\int\limits_{0}^{\xi_{(s)}} \exp\left(-\frac{\xi^2}{4\eta_{(1)}}\right)d\xi\right]^{-1}, \\ T_{(1)} = T_{(s)} + \left(T_e - T_{(s)}\right)\int\limits_{\xi}^{\xi_{(s)}} \exp\left(-\frac{\xi^2}{4} - \frac{\mathrm{Pe}_{(1)}}{2p_0^2}p_{(1)}^2\right)d\xi \left[\int\limits_{0}^{\xi_{(s)}} \exp\left(-\frac{\xi^2}{4} - \frac{\mathrm{Pe}_{(1)}}{2p_0^2}p_{(1)}^2\right)d\xi\right]^{-1}, \end{cases} \quad 0 < \xi < \xi_{(s)}; \qquad (4)$$

$$\begin{cases} p_{(2)}^2 = p_{(0)}^2 + \left(p_{(s)}^2 - p_0^2\right)\int\limits_{\xi}^{\infty} \exp\left(-\frac{\xi^2}{4\eta_{(2)}}\right)d\xi \left[\int\limits_{\xi_{(s)}}^{\infty} \exp\left(-\frac{\xi^2}{4\eta_{(2)}}\right)d\xi\right]^{-1}, \\ T_{(2)} = T_0 + \left(T_{(s)} - T_0\right)\int\limits_{\xi}^{\infty} \exp\left(-\frac{\xi^2}{4} - \frac{\mathrm{Pe}_{(2)}}{2p_0^2}p_{(2)}^2\right)d\xi \left[\int\limits_{\xi_{(s)}}^{\infty} \exp\left(-\frac{\xi^2}{4} - \frac{\mathrm{Pe}_{(2)}}{2p_0^2}p_{(2)}^2\right)d\xi\right]^{-1}, \end{cases} \quad \xi_{(s)} < \xi < \infty. \qquad (5)$$

According to the conditions (3), with regard to the solutions (4) and (5), the coordinate of the phase boundary $\xi_{(s)}$ and the parameters $p_{(s)}$ and $T_{(s)}$ on this boundary are given by

$$\left(p_e^2 - p_{(s)}^2\right)\exp\left(-\frac{\xi_{(s)}^2}{4\eta_{(1)}}\right)\left[\int\limits_{0}^{\xi_{(s)}} \exp\left(-\frac{\xi^2}{4\eta_{(1)}}\right)d\xi\right]^{-1} = \frac{m\mu_{g(1)}\chi^{(T)}p_{(s)}}{k_{g(1)}}\left(\frac{\rho_h G S_h}{\rho_{g0}} + 1 - S_h\right)\xi_{(s)}; \qquad (6)$$

$$\left(p_{(s)}^2 - p_0^2\right)\exp\left(-\frac{\xi_{(s)}^2}{4\eta_{(2)}}\right)\left[\int\limits_{\xi_{(s)}}^{\infty} \exp\left(-\frac{\xi^2}{4\eta_{(2)}}\right)d\xi\right]^{-1} = \frac{m\mu_{g(2)}\chi^{(T)}p_{(s)}}{k_{g(2)}}\left(1 - S_{i0}\right)\xi_{(s)}; \qquad (7)$$

$$\left(T_{(s)} - T_e\right)\exp\left(-\frac{\xi_{(s)}^2}{4} - \frac{\mathrm{Pe}_{(1)}}{2p_0^2}p_{(s)}^2\right)\left[\int\limits_{0}^{\xi_{(s)}} \exp\left(-\frac{\xi^2}{4} - \frac{\mathrm{Pe}_{(1)}}{2p_0^2}p_{(1)}^2\right)d\xi\right]^{-1} -$$

$$-\left(T_0 - T_{(s)}\right)\exp\left(-\frac{\xi_{(s)}^2}{4} - \frac{\mathrm{Pe}_{(2)}}{2p_0^2}p_{(s)}^2\right)\left[\int\limits_{\xi_{(s)}}^{\infty} \exp\left(-\frac{\xi^2}{4} - \frac{\mathrm{Pe}_{(2)}}{2p_0^2}p_{(2)}^2\right)d\xi\right]^{-1} = \frac{m\rho_h L_h S_h}{\rho c}\xi_{(s)}. \qquad (8)$$

To solve the resulting system of equations, the pressure $p_{(s)}$ is expressed from (6) and substituted into (7), which leads to the transcendent equation with respect to a single unknown $\xi_{(s)}$ (solved by the bisection method in this study); then the pressure $p_{(s)}$ and the temperature $T_{(s)}$ at the boundary $\xi_{(s)}$ are found by equations (6) and (8).

Regimes of gas hydrate formation

Gas hydrates form with the release of latent heat of phase change, which interferes with the temperature pattern of the porous reservoir we model. The obtained solutions have been checked for thermodynamic consistency requiring the local temperature in domain 1 to be lower than the temperature of CO_2 hydrate decomposition found from the pressure distribution according to our solution (i) and the local temperature in domain 2 to be below 273 K or the ice melting point (ii).

Temperature and pressure variations along the coordinate x were plotted for different pressures p_e of injected CO_2 at the time t = 3.5 hr (Fig. 3), for a system with the parameters m = 0.2; p_0 = 1.15 MPa; T_0 = 271 K; S_{i0} = 0.6; T_e = 271 K; $k_0 = 2\cdot10^{-15}$ m^2; ρ_{sk} = 2400 kg/m^3; ρ_i = 900 kg/m^3; ρ_h = 1100 kg/m^3; G = 0.28; $R_{g(1)}$ = 189 J/(K·kg); $R_{g(2)}$ = 520 J/(K·kg); $\mu_{g(1)} = 1.3\cdot10^{-5}$ Pa·s; $\mu_{g(2)} = 10^{-5}$ Pa·s; $c_{g(1)}$ = 800 J/(K·kg); c_{sk} = 1200 J/(K·kg); $c_{g(2)}$ = 1560 J/(K·kg); c_i = 2100 J/(K·kg); $\rho c = 2.5\cdot10^6$ J/(K·m^3); λ = 2 W/(m·K); p_{s0} = 1.02 MPa; T_{*glh} = 7.6 K; T_{*gih} = 19 K.

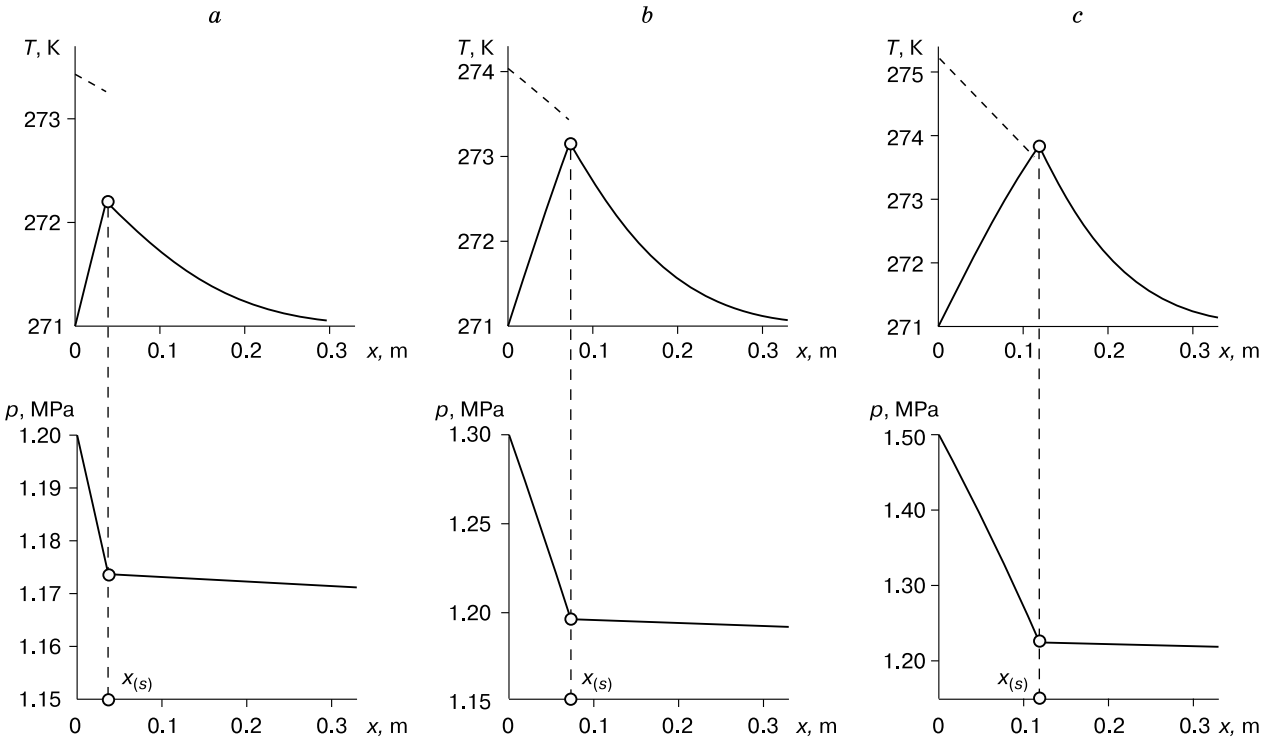

Fig. 3. Variations of reservoir temperature T and pressure p along the coordinate x at different pressures of injected CO_2: p_e = 1.2 MPa (a), p_e = 1.3 MPa (b), and p_e = 1.5 MPa (c).

Dash lines are equilibrium temperatures of CO_2 hydrate formation corresponding to calculated pressures.

The specific heat of the ice-CO_2 hydrate transition per hydrate unit mass is assumed to be $L_h = 1.6 \cdot 10^5$ J/kg [*Anderson, 2003*]. Dash lines show equilibrium temperatures of CO_2 hydrate formation corresponding to the calculated pressures. At relatively small gas injection pressures (with respect to the other values used in calculations), the reservoir temperature is below the equilibrium temperature of CO_2 hydrate decomposition in domain 1 and below the ice melting point in domain 2 (Fig. 3, *a*). Thus, the solution with a single phase transition front (phase boundary) faithfully describes the hydrate formation process.

At higher pressures of injected gas (Fig. 3, *b*), the reservoir temperature beyond the phase boundary (domain 2) rises above 273 K in local zones where ice should melt. Thus, there arise another phase boundary and another domain saturated with methane and water (Fig. 4).

Further increase in the injected gas pressure (Fig. 3, *c*) leads to reservoir temperature rise above the equilibrium temperature of CO_2 hydrate decomposition within some part of domain 1, where the mixture of gaseous and hydrate carbon dioxide thus becomes overheated. It means the existence of one more phase boundary and, correspondingly, another domain, saturated with carbon dioxide and water, between the CO_2 + gas hydrate and CH_4 + water domains (Fig. 5).

Gas hydrate formation with two phase boundaries and three domains occurs at $T_{(s)} > 273$ K on the boundary $\xi_{(s)}$, where $T_{(s)}$ is the temperature at the

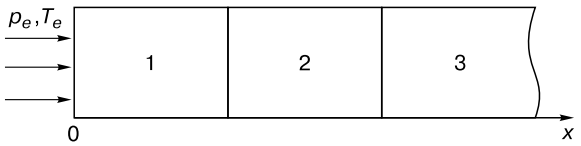

Fig. 4. Gas hydrate formation with two phase boundaries.

1 – saturation with CO_2 hydrate and free carbon dioxide; 2 – saturation with water and methane; 3 – saturation with ice and methane.

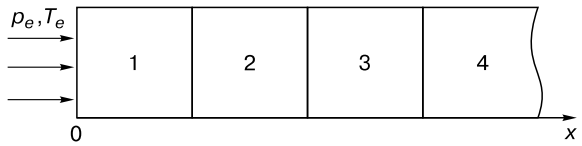

Fig. 5. Gas hydrate formation with three phase boundaries.

1 – saturation with CO_2 hydrate and free carbon dioxide; 2 – saturation with water and carbon dioxide; 3 – saturation with water and methane; 4 – saturation with ice and methane.

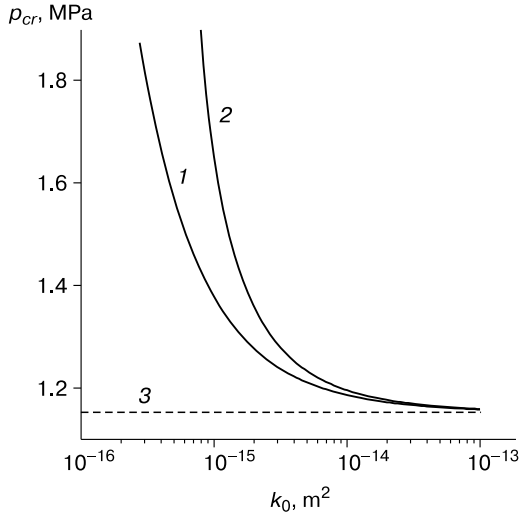

Fig. 6. Critical pressure of injected CO_2 (p_{cr}) as a function of reservoir permeability k_0.

1 – two phase boundaries; *2* – three phase boundaries; *3* – initial reservoir pressure.

phase boundary found by (8). Three phase boundaries and four domains arise at $T_{(s)} > T_{(1)s}$ on the boundary $\xi_{(s)}$, where $T_{(1)s}$ is the temperature of gas hydrate decomposition found by (1) corresponding to the pressure $p_{(s)}$.

These inequalities were used in numerical experiments with large ranges of parameters in order to find such critical injected gas pressure p_{cr} above which two or three phase boundaries arise in the gas hydrate formation process. The calculations showed that the p_{cr} value depends mainly on the permeability and initial pressure of the reservoir.

The permeability dependences of gas injection pressure that control the gas hydrate formation regimes have been plotted for the same initial temperature of the injected gas and the reservoir (Fig. 6). Other parameters in the plots of Fig. 6 are as in Fig. 3. Dash line *3* parallel to the x axis (the horizontal asymptote of the solid curves) shows the initial reservoir pressure. The critical pressure p_{cr} decreases with permeability (Fig. 6), and gas injection into poorly permeable porous rocks at low p_e produces two domains of CO_2 + gas hydrate and CH_4 + ice. Progressive increase in injected gas pressure or reservoir permeability gives rise, successively, to the third and fourth domains saturated with methane + water (domain 3) and carbon dioxide + water (domain 4).

As shown by plots in Fig. 7 for two different CO_2 injection pressures, the temperature at the phase boundary and its self-similar coordinate increase proportionally to permeability, and the rate of this increase is faster at higher gas pressures. Therefore, the results presented in Figs. 3 and 6 can be explained by release of latent hydrate formation heat. Inasmuch as the rate of phase transition is controlled by mass transfer in the reservoir, gas injection pressure or permeability increase leads to faster gas hydrate formation and, hence, to greater heat release. The heat released at very fast hydrate formation exceeds the heat loss and causes ice melting creating domains saturated with gas (CO_2 or CH_4) and water.

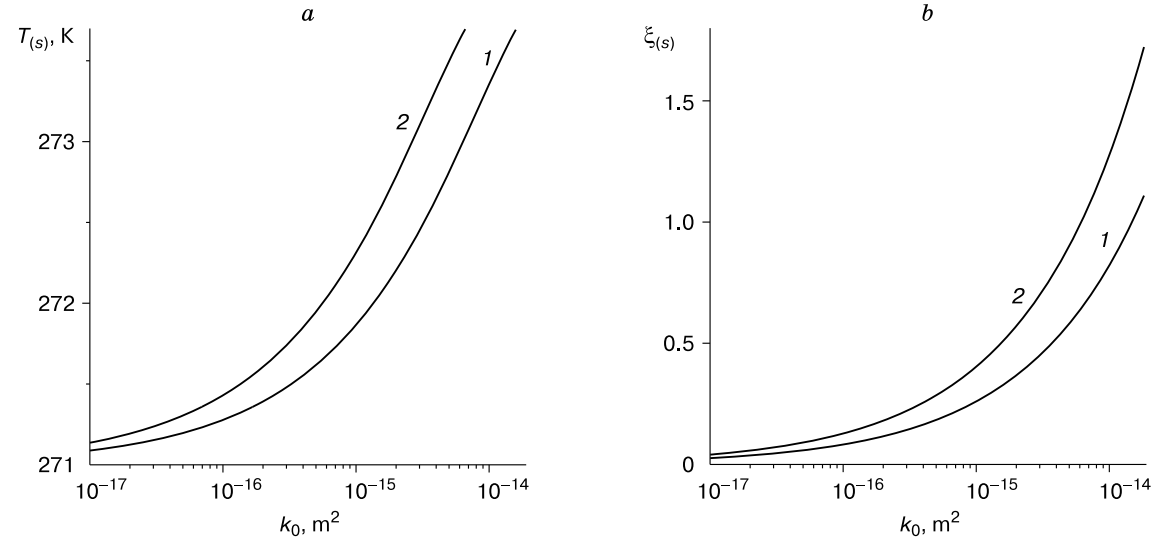

Fig. 7. Temperature $T_{(s)}$ at phase boundary (*a*) and self-similar coordinate $\xi_{(s)}$ of phase boundary (*b*) as a function of reservoir permeability k_0 at different pressures of injected gas: p_e = 1.2 MPa (*1*) and p_e = 1.25 MPa (*2*).

CONCLUSIONS

We have modeled the formation of CO_2 hydrate by injection of gaseous carbon dioxide into an ice-rich methane reservoir and obtained self-similar solutions in a plane-parallel approximation for reservoir pressure and temperature. The solutions show gas hydrate formation with one, two, or three phase boundaries, depending on the pressure of injected CO_2 and the reservoir permeability. Correspondingly, injection at a low pressure into a poorly permeable methane reservoir produces two domains with gaseous CO_2 + hydrate CO_2 and ice + methane. As the gas injection pressure and the reservoir permeability progressively increase, ice melting caused by heat excess gives rise to additional domains of methane + water (domain 3) and then CO_2 + H_2O (domain 4).

Therefore, it is possible to avoid CO_2 hydrate decomposition and risks posed by ice melting to mechanic strength of rocks by maintaining relatively low pressure of CO_2 injection, especially in the case of high reservoir permeability. These results have implications for the choice of strategies that secure subsurface CO_2 sequestration and its safe disposal as gas hydrate in porous reservoirs, as well as for the conditions of CO_2 hydrate stability.

The study was supported by grant SS-6987.2016.1 from the Grant Council of the President of the Russian Federation for Support of Leading Science Schools.

References

Anderson, G.K., 2003. Enthalpy of dissociation and hydration number of carbon dioxide hydrate from the Clapeyron equation. J. Chem. Thermodynamics 35, 1171–1183.

Barenblatt, G.I., Entov, V.M., Ryzhik, V.M., 1982. Flow of Liquids and Gases in Natural Rocks. Nedra, Moscow, 211 pp. (in Russian)

Basniev, K.S., Basniev, K.S., Kochina, I.N., Maksimov, V.M., 1993. Subsurface Fluid Mechanics. Nedra, Moscow, 416 pp. (in Russian)

Benson, S.M., Cole, D.R., 2008. CO_2 sequestration in deep sedimentary formations. Elements 4, 325–331.

Byk, S.Sh., Makogon, Yu.F., Fomina, V.I., 1980. Gas Hydrates. Khimiya, Moscow, 296 pp. (in Russian)

Chuvilin, E.M., Guryeva, O.M., 2008. Carbon dioxide gas hydrates accumulation in freezing and frozen sediments, in: Proc. 6th Intern. Conf. on Gas Hydrates. Vancouver, Canada, No. 5469.

Chuvilin, E.M., Guryeva, O.M., 2009. Experimental investigation of CO_2 gas hydrate formation in porous media of frozen and freezing sediments. Kriosfera Zemli XIII (3), 70–79.

Chuvilin, E.M., Petrakova, S.Y., Guryeva, O.M., Istomin, V.A., 2007. Formation of carbon dioxide gas hydrates in freezing sediments and decomposition kinetics of the hydrates formed, in: Kuhs, W.F. (Ed.), Physics and Chemistry of Ice, Cambridge, UK, Roy. Soc. Chemistry, pp. 147–154.

Duchkov, A.D., Sokolova, L.S., Ayunov, D.E., Permyakov, M.E., 2009. Assessment of potential of West Siberian permafrost for the carbon dioxide storage. Kriosfera Zemli XIII (4), 62–68.

Istomin, V.A., Yakushev, V.S., 1992. Gas Hydrates in Nature. Nedra, Moscow, 236 pp. (in Russian)

Jadhawar, P., Mohammadi, A., Yang, J., Tohidi, B., 2006. Subsurface carbon dioxide storage through clathrate hydrate formation, in: Advances in the Geological Storage of Carbon Dioxide, Springer, Print, Netherlands, pp. 111–126.

Khasanov, M.K., Gimaltdinov, I.K., Stolpovsky, M.V., 2010. Specific features of the formation of gas hydrates during the injection of a cold gas into a porous medium saturated with a gas and water. Theoretical Foundations of Chemical Engineering 44 (4), 424–431.

Komai, T., Sakamoto, Y., Kawamura, T., et al., 2008. Formation kinetics of CO_2 gas hydrates in sandy sediment and change of permeability during crystal growth – carbon capture and storage system using gas hydrates, in: Proc. 6th Intern. Conf. on Gas Hydrates, Vancouver, Canada, No. 5342.

Makogon, Yu.F., 1974. Hydrates of Natural Gases. Nedra, Moscow, 208 pp. (in Russian)

Nigmatulin, R.I., 1987. Dynamics of Multiphase Media. Part 2. Nauka, Moscow, 360 pp. (in Russian)

Oldenburg, C.M., Pruess, R., Benson, S.M., 2001. Process modeling of CO_2 injection into natural gas reservoirs for carbon sequestration and enhanced gas recovery. Energy and Fuel 15, 293–298.

Olovin, B.A., 1993. Infiltration Permeability of Permafrost. Nauka, Novosibirsk, 257 pp. (in Russian)

Shagapov, V.Sh., Khasanov, M.K., Musakaev, N.G., 2008. Formation of a gas hydrate due to injection of a cold gas into a porous reservoir partly saturated by water. Journal of Applied Mechanics and Theoretical Physics 49 (3), 462–472.

Shagapov, V.Sh., Khasanov, M.K., Gimaltdinov, I.K., Stolpovsky, M.V., 2011. Numerical modeling of formation of a gas hydrate in a finite-length porous bed purged by a gas. Journal of Applied Mechanics and Theoretical Physics 52 (4), 116–126.

Shagapov, V.Sh., Musakaev, N.G., Khasanov, M.K., 2015. Formation of gas hydrates in a porous medium during an injection of cold gas. Intern. J. Heat and Mass Transfer 84, 1030–1039.

Tsypkin, G.G., 2014. Mathematical model of carbon dioxide injection into rocks with formation of gas hydrate. Doklady Earth Sci. 458 (4), 422–425.

Yakushev, V.S., Perlova, E.V., Makhonina, N.A., Chuvilin, E.M., Kozlova, E.V., 2003. Gas hydrates in deposits of continents and islands. Rossiiskiy Khimicheskiy Zhurnal XLVII (3), 80–90.

Received February 24, 2015